Shape Selective Nano-Catalysts: Toward Direct Methanol Fuel Cells Applications

Simona E. Hunyadi Murph [1*] and Ricardo D. Torres[1]

[1]Savannah River National Laboratory,
Aiken, SC, 735-11A, Room 125
[*]Simona.Murph@srnl.doe.gov

ABSTRACT

A series of bimetallic core-shell-alloy type Au-Pt nanomaterials with various morphologies, aspect ratios and compositions, were produced in a heterogenous epitaxial fashion. Gold nanoparticles with well-controlled particle size and shape, e.g. spheres, rods and cubes, were used as "seeds" for platinum growth in the presence of a mild reducing agent, ascorbic acid and a cationic surfactant cethyltrimethyl ammonium bromide (CTAB). The reactions take place in air and water, and are quick, economical and amenable for scaling up. The synthesized nanocatalysts were characterized by electron microscopy techniques and energy dispersive X-ray analysis. Nafion membranes were embedded with the Au-Pt nanomaterials and analyzed by atomic force microscopy (AFM) and scanning electron microscopy (SEM) for their potential in direct methanol fuel cells applications.

Keywords: nanoparticles, gold-platinum core-shell/alloy, Nafion.

1 INTRODUCTION

Direct methanol fuel cells (DMFCs) have recently attracted much interest as a promising alternative to conventional batteries, especially in portable electronic devices. The main advantages for the use of methanol as fuel are its high energy density and its liquid state at room temperature. Currently, Pt and Pt alloys catalyst are the most effective catalysts for methanol electro-oxidation in DMFCs [1]. Depending on the alloy composition, the catalyst size, shape, surface structure, reaction site distribution (e.g. planar, edge, and corner) or oxidation state, different catalytic activities are achievable. DMFCs, however, have several disadvantages including high cost resulting from high precious metal catalyst load requirements, slow kinetics due to adsorbed carbon monoxide (CO) during one of the intermediate steps [2] and methanol crossover.

Pt-modified Au electrodes have attracted much interest due to their high activity and stability in methanol electro-oxidation [3]. For example, Mihut at al. [4] showed that catalysts prepared by impregnation from Pt and Au precursors exhibited a lower activation energy, facilitating the oxidative desorption and suppressing the adsorption of CO.

Bimetallic nanoparticles have also received great attention due to their novel catalytic, electronic, and optical properties, which are distinct from either of their constituent monometallic nanoparticles; the presence of another metal atom in the original lattice affects its composition, crystal structure and electronic structure [1,5, 6]. Zeng et al. reported that the CO-stripping peak of core–shell Au–Pt nanoparticles occurs at a more negative potential than that of pure Pt nanoparticles. This indicated that the interface between the Pt shell and the Au core was effective at removing CO adsorbed on Pt [7]. Moreover, CO peak positions were dependent on the level of Pt coverage on the Au substrate [8].

While there are numerous studies on the use of Pt and Pt-alloys spherical nanoparticles for fuel cells applications [1], there are limited reports on bimetallic Au-Pt nanoparticles with controllable shape, size and composition [9]. Evidence supports that nanoparticle shape is critical in catalytic reactions. For example, El-Sayed reported the use of platinum tetrapod shaped nanoparticles to catalyze the Suzuki cross-coupling reaction [10]. While spherical Pt nanopartices do not catalyze this reaction, tetrapod-shaped nanoparticles will while undergoing a shape change into spheres. This suggested that the ends of the tetrapods were significantly more reactive than their cores.

Typical methods of manufacturing electrode–membrane assemblies for fuel cells involve painting, spraying, or printing of the catalyst. However, these methods are limited on the effective distribution of Pt catalysts at the three-phase interface region (catalyst/carbon /electrolyte), which allows for effective proton, electron and gas transport to and from the catalyst sites. Nafion, a negatively charged polymer with sulfonic acid groups, is one of the most widely used membranes for DMFCs due to its good thermal and chemical stability and high proton conductivity. One effective strategy to improve catalyst loading, its distribution and utilization is direct embedding of the Nafion membrane with the nanoparticles. Preliminary studies by Jiang [11] reported that poly(diallyldimethyl ammonium chloride) PDDA-stabilized Pt spherical nanoparticles can also block the methanol crossover through the Nafion electrolyte membrane while enhancing the performance of the DMFC.

In this paper, we describe a wet chemical approach for the synthesis of four different shaped bimetallic core-shell-alloy type Au-Pt nanoparticles trough a hetero-epitaxial approach. Tunable Au nanoparticles, e.g. spheres, rods and cubes were prepared by a seed mediated approach [12,13] and used as templates. The shapes of the Au-Pt nanoparticles, including hexagons, rods, 'dogbones' and cubes, were controlled by changes in the concentration of reactants in the reduction synthesis procedure. Subsequently, platinum-gold nanomaterials were embedded and self-assembled into Nafion membranes deposited by drop casting.

2 EXPERIMENTAL SECTION

Chloroauric acid trihydrate, silver nitrate, potassium tetrachloroplatinate (II), cetyltrimethylammonium bromide (CTAB), sodium borohydride and ascorbic acid were purchased from Sigma Aldrich. All chemicals were used as received. All glassware was cleaned with aqua regia, and thoroughly rinsed with deionized water prior to use.

Gold nanoparticles, including cubes, spheres and rods of different aspect ratios were prepared from seed-mediated surfactant-directed approaches described in our previous reports [1,14]. The as prepared rods were either (a) purified by centrifugation and redispersed in DI water to remove the unreactive reactants or (b) unpurified and used "as is" for production of Au-Pt nanomaterials. Bifunctional Au-Pt nanoparticles were prepared by mixing 5 ml of Au nanorod solutions (a) or (b) with 10 ml of 0.1 M cetyltrimethyl ammonium bromide (CTAB) aqueous solution followed by addition of 78.5mM K_2PtC_{l6}, and 157µl of 0.1M AA. The two solutions were stirred at 40°C for 12 hours. Polymer membranes were produced by codepositing solutions of Nafion™/ethanol (20% by wt.) and the catalysts (30 µL, each) via drop casting on silicon wafers. The membranes were dried at room temperature.

3 RESULTS AND DISCUSSIONS

3.1 Catalyst Synthesis and Characterization

A series of anisotropic core-shell-alloy type Au-Pt nanoparticles were prepared in a heterogenous epitaxial fashion, with the use of Au nanoparticles as "seeds" for platinum growth [1]. The Au nanoparticle "seeds" library consisted of tunable Au nanoparticles, spheres, rods and cubes that were produced by a seed mediated approach as reported earlier by us (Figure 1) [12, 13]. Figure 1 shows TEM images of the Au nanoparticle library, including spheres, different aspect ratio rods and cubes that were used as templates for the production of bimetallic Au-Pt substrates.

These reactions take place in air, and water, at 40°C temperature, and, in principle, are amenable for scaling up. Growth solutions containing a Pt metal salt, "Au seed solution," a structure-directing agent, and a weak reducing agent (ascorbic acid), produced core-shell alloy type nanoparticles with different morphologies [1]. CTAB has been used as a capping reagent to avoid aggregation. Small changes in reaction conditions (seed to metal ratio, absence of Ag ions, etc.) were used to control the final morphology, size and shape of the gold nanoparticles (Figure 1).

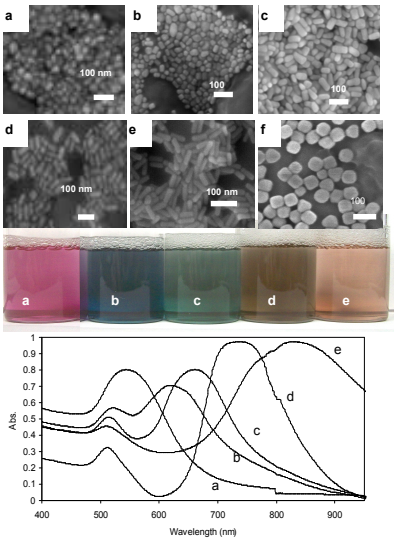

Figure 1. Electron micrographs images (a-f), photographs, and UV-Vis spectra of Au nanoparticles (a) spheres, (b-e) different aspect ratios rods, and (f) cubes.

Growth of the Pt shell onto the Au nanotemplate was monitored via x-ray energy dispersive microanalysis (EDX), electron microscopy (TEM and SEM) and UV-visible absorption spectroscopy.

EDX and mapping analysis of the bimetallic colloids was performed, which revealed the final composition and distribution of Pt on the Au template. The mapping analyses of all anisotropic Au-Pt nanoparticles confirmed that the Pt coating is distributed entirely on the Au template (data not shown on all nanomaterials). A representative EDX mapping of Au-Pt hexagons is shown in Figure 2; the red spots represent Pt while green spots represent Au.

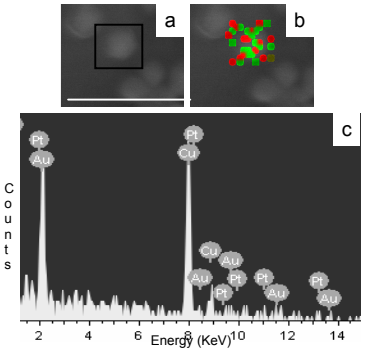

Figure 2. (a) Electron micrograph (b) Au-green and Pt-red elemental map (c) EDX analysis of Au-Pt hexagons;, Scale bar: 200

The Au nanoparticle "seeds" were used in both purified and unpurified form for the growth. Depending on the reaction procedure, Au-Pt nanoparticles with different morphologies, uniformity and surface smoothness were produced. Figure 3 shows electron micrographs of Au-Pt bimetallic nanoparticles, such as hexagons, cubes,

'dogbones' and rods. While the final geometry and surface appearance varied based on the reaction parameters, in all cases the initial morphology of the Ag nanowires was preserved and the size of the growing platinum shell was determined by the original diameter of the Au "seeds." We found that the purification steps used in the synthesis procedure and the Au template shapes are critical for the production of either uniform or porous bimetallic structures with a core-shell-alloy type morphology (Figure 3).

Surprisingly, when Au spheres were unpurified and used "as is," novel hexagonal shaped bimetallic structures were produced, exhibiting smooth surfaces and uniform outer shells. The initial Au nanosphere core size, with an average diameter of 28±2 nm, increased to a 49±2nm diameter for Au-Pt hexagons, with a 42±2nm diagonal length (Table 1). In parallel experiments, Au-Pt nanocubes (Figure 3b) were prepared by a similar approach, but purified Au cubes (56±2nm) libraries were used (Figure 1f, Table 1). In this case, the Au-Pt cubes retained a similar morphology to the original Au cubic template, but with a slightly more "rounded" appearance. This suggests that Pt growth is selectively faster on the facets and not on the tips of the cubes, resulting in a more "rounded" morphology. The Pt outer shell was smooth and uniform.

Table 1. Template and catalyst dimensions in nm

Substrate	Length (nm)	Width (nm)	Diameter (nm)
Au spheres	-	-	28±2
Au-Pt hexagons	-	42±2	49±2
Au rods	72±2	22±1	-
Au-Pt 'dogbones'	81±3	34±2	-
Au-Pt rods	75±1	24±2	-
Au cubes	-	-	56±2
Au-Pt cubes	-	-	69±2

Different aspect ratio Au nanorods were used as template for the production of Au-Pt colloids by using either purified or unpurified Au colloids. In both cases, the TEM images revealed the formation of distinct Pt protuberances and islands on the Au nanorods "seed" surfaces in a core-shell-like arrangement. However, 'dogbone' structures or rod-like nanostructures were produced by altering the procedure. When purified Au nanorods were used, TEM images showed a more uniform coating along the whole surface with more Pt-islands at the end of the rods (Figure 3). The initial morphology of the Au nanorods was preserved and the size of the growing Au-Pt nanoparticles was determined by the original diameter of the Au nanorods. Alternatively, when unpurified Au nanorods were used dogbone-like Au-Pt colloids were produced. This is not surprising since just ~15% of the initial gold ions in the growth solution are reduced to form nanorods [12]. Additional reducing agent resulted in preferential deposition of more Au at the end of the rods that yield "dogbone'-like structure [12, 13, 14].

UV-vis spectra were used to monitor morphological changes during the Pt deposition on the Au template. Anisotropic metal nanoparticles can absorb and scatter light along multiple axes; therefore, metal nanorods and nanowires have both longitudinal (long axis) and transverse (short axis) plasmon bands (Figure 1).

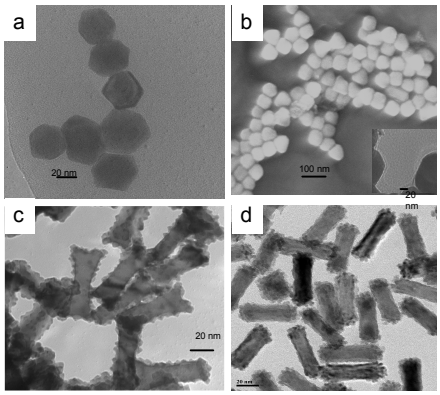

Figure 3. Electron micrographs of Au-Pt (a)hexagons, (b) cubes, (c) dogbones, (d) rods.

In the case of gold nanoparticles, surface plasmon bands appear in the visible region of the spectrum and are very sensitive to particles size, shape, environment and dielectric constant (Figure 1). For example, the plasmon band of gold nanospheres, occurs at ~520 nm, while in nanorods two plasmon bands were observed from ~500nm to ~1000nm, each dependent on the nanorod aspect ratio. Coating the nanoparticles with materials of different dielectric constant shifts the the plasmon band positions in ways that are readily identifiable spectroscopically as well as theoretically understood [12,14,]. The overgrowth of Pt deposits on the Au nanorods (Table 2) induces a red shift of the longitudinal band for all samples, except for the Au-Pt cubes, where a blue shift was recorded.

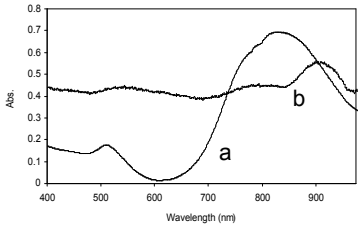

Figure 4. UV-Vis spectra of (a) Au rods and (b) Au-Pt 'dogbones.'

Table 2. Summary of UV-Vis spectra plasmon bands.

Substrate	Transverse plasmon band (nm)	Longitudinal plasmon band (nm)	Plasmon band(nm)
Au spheres vs. Au-Pt hexagons	-	-	528-537
Au cubes vs. Au-Pt cubes	-	-	539-524
Au rod vs. Au-Pt 'dogbones'	507-537	827-903	-
Au rods vs. Au-Pt rods	512-516	661-691	-

3.2 Catalyst Embedding in Nafion

A self-assembly approach, based on electrostatic interactions between the positively-charged Au-Pt particles (as revealed by ζ measurements [12,14]; data not shown) and the negatively-charged Nafion's sulfonic acid groups was used to produce the Pt modified Nafion membrane. Since the nanoparticles sizes are <100 nm, it is difficult to distinguish the different shapes. However, the SEM images (Figure 5) shows that the nanocatalysts were well dispersed inside the membrane, with no clusters or aggregates.

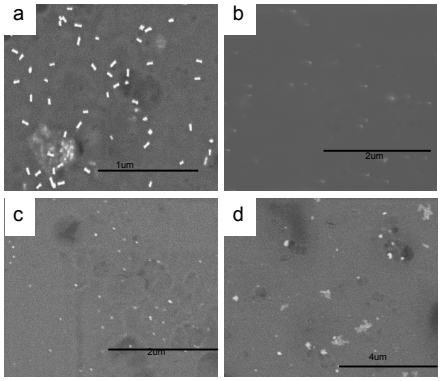

Figure 5. SEM images of Au-Pt nano-catalyst impregnated Nafion membranes (a) dogbone, (b) rods, (c) hexagons, (d) cubes.

Atomic force microscopy (AFM) was used to characterize the topography of the Nafion polymer films embedded with nanoparticles. All images were obtained with a Veeco Multimode AFM operated by tapping mode. Figure 6a,b show representative AFM images from a film embedded with Au-Pt nanorods. Each image corresponds to a different area in the same film. The Au-Pt nanorods were not observed at the film surface indicating that they were fully embedded within the matrix polymer. Topography measurements yielded RMS roughness of ~2-4 nm, although drop-casting produced surface artifacts upon drying (not shown), which resulted in substantially higher roughness in some sections. Surface 'valleys' could be observed from what preliminarily appears to be the film contracting as the casting solvent evaporated. Further studies will focus on characterizing film thickness (profilometry) at different polymer-solution concentrations and optimizing film quality by spin-coating.

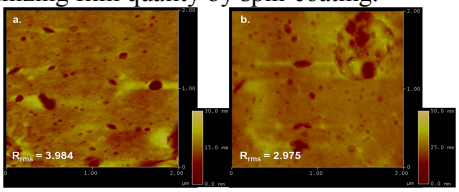

Figure 6. AFM topographic images of Nafion polymer films embedded with Pt-Au nanorods.

Figure 7a shows an AFM image of a Nafion polymer film embedded with Au-Pt-Ag nanohexagons. The film topography appeared similar to the films on, although some particles could be traced on the surface (Figure 7b). It is possible that the different particle shapes and composition exhibit varying buoyant properties in the polymer while it remains swollen. As a result, different shaped particles lead to varied surface density.

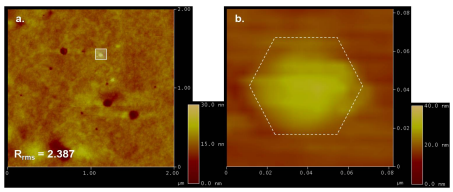

Figure 7. AFM topographic images of a) Nafion polymer film embedded with Pt-Au-Ag nanohexagons; b) Protruding nanohexagon at surface.

4 CONCLUSIONS**

We produced a series of tunable Au-Pt bimetallic colloids with distinctive optical properties, morphology, size, shape and surface porosity by a simple hetero-epitaxial approach. These nanomaterials were efficiently self-assembled by direct embedding into Nafion membranes and will be further explored for fuel cells applications.

** We thank Dr. E. Fox for the use of AFM and Savannah River National Laboratory LDRD-DOE for funding.

REFERENCES

[1] S.E. Hunyadi Murph, S. Serkiz, E. Fox..and H. Colon-Mercado, et al. Book Chapter ACS Symposium Series Volume, 2010, accepted and references herein.
[2] U.A. Paulus, U. Endruschat and G. J. Feldmeyer, et al *J. Catal*. 195, 383, 2000.
[3] J.H. Zeng, J. Yang, J.Y. Lee and W.J. Zhou, J. Phys. Chem. B 110, 24606, 2006.
[4] C. Mihut, C. Descorme, D. Duprez and M. Amiridis, J. Catal. 212, 125, 2002.
[5] S.E. Hunyadi, C.J. Murphy, J. Cluster Science, 20, 319, 2009.
[6] S.E. Hunyadi, C.J. Murphy, *J. Mater. Chem.* 16, 3929, 2006.
[7] J.H. Zeng, J. Yang, J.Y. Lee and W.J. Zhou, J. Phys. Chem. B 110, 24606, 2006.
[8] I.S. Park, K.S. Lee, Y.H. Cho, H.Y Park and Y.E Sung Catalysis Today 132, 127, 2008.
[9] S. Guo, J. Colloid and Interface Science, 35, 363, 2007.
[10] R. Narayanan and M.A. El-Sayed, *Langmui*r, 21, 2027, 2005.
[11] P.S. Jiang, Z. Liu, H.L. Tang, and M. Pan, Electrochimica. Acta, 51, 5721, 2006.
[12] C.J. Murphy, T.K. Sau, S.E. Hunyadi, et al J. Phys. Chem. B, 109, 13857, 2005; ; and references herein.
[13] C.J. Murphy, A.M. Gole and S.E. Hunyadi, Inorg. Chem. 45, 7544, 2006; and references herein
[14] C.J. Murphy, A.M. Gole and S.E. Hunyadi et al Chem. Comm., 4, 554, 2008; and references herein.